IEEE Robotics and Automation Letters (RAL) paper presented at
2024 IEEE/RSJ International Conference on Intelligent Robots and Systems (IROS)
October 14-18, 2024. Abu Dhabi, UAE

How fast can a robotic drummer beat using dielectric elastomer actuators?

Sudhir Wakle[1], Tze-Han Lin[2], Shu Huang[3], Sumit Basu[4], and Gih-Keong Lau[5*]

***Abstract*— Fast drumming presents a speed challenge to many robotic arms. To meet the simultaneous needs for speed, stroke, and force, we proposed and tested a new double-saddle dielectric elastomer actuator (DEA) as the artificial biceps for driving a lightweight robotic drummer. This work finds that fast force induction is instrumental to the fast drumming by a DEA-supported drumstick that makes a pivoted forearm. While a large pre-stretch and lateral reinforcement in a pure-shear series of DEA was good for generating a large isotonic stroke, it is not fast in isometric force induction. Instead, this work found a double-saddle DEA, which is a degenerated two-segment pure-shear DEA with a middle laterally buckled beam, managed to induce fast isometric force at down time constant of 0.5s when its ultimate actuation tapered due to substantial strain stiffening effect. As such, this double-saddle DEA-driven drummer suffered a less dynamic stroke decrement than the 8-segment DEA did. A 4.4-gram DEA managed to swing freely a 7.8-gram drumstick up to nearly 60 degrees at 5.5-6kV and a maximum tip speed of up to 0.45m/s. The drumming frequency upon 5.5kV activation was up to 2-2.5Hz. In comparison, an 8-segment pure-shear DEA-driven drummer fail to reach the drum when pulsed at 2Hz. Interestingly, a slower stroke can excite multiple drumbeats due to secondary bounces. To achieve a faster drumming to match human drummer, it is foreseen that a harder dielectric elastomer material will help drive a faster soft robot.**

I. Introduction

How fast can a drummer beat? The 2022 Guinness Word records[1] declared that an 11-year-old Australian boy is the world's fastest drummer; he managed to beat a drum with drumsticks as fast as 39.5 times per second. This means nearly 20 drum beats per second by a single hand, well exceeding the bandwidth of neuromuscular stimuli of 10 Hz. According to Ref. [2], [3], [4], a human drummer can often play the drum rolls (with a bounce interval between 30 ms and 140 ms) at a grasp force between 3 N to 36 N. Then, skilled drummers can beat fast by taking the advantage of a passive dynamic interaction; the drumstick bounces at least twice with each hand stroke.

IROS Submission 61: Presentation of IEEE RAL Paper 10.1109/LRA.2024.3357034

[1]Sudhir Wakle with International College of Semiconductor Technology, National Yang Ming Chiao Tung University, Hsinchu, Taiwan and Mechanical Engineering Department, Indian Institute of Technology Kanpur, India and spwakle@iitk.ac.in

[2]Tze-Han Lin with Department of Graduate Degree Program of Robotics, National Yang Ming Chiao Tung University, Taiwan 30010

[3]Shu Huang with Mechanical and Mechatronics System Research Labs, Industrial Technology Research Institute, Taiwan 31057

[4]Sumit Basu with Mechanical Engineering Department, Indian Institute of Technology Kanpur, India

[5*]Gih-Keong Lau with Department of Mechanical Engineering and International College of Semiconductor Technology, National Yang Ming Chiao Tung University, Taiwan 30010 mgklau@nycu.edu.tw

After this human drumming technique, Harvard researchers[2] in 1997 developed a single-joint drumming robot using a pair of McKibben pneumatic artificial muscles. Their drumming robot managed to play the drum rolls as fast as a human drummer despite that the pneumatic drive took 93 ms rise time to raise the drumstick by 53 mm high. Meanwhile, MIT researchers [3] demonstrated the stick bounces were controllable by applying an oscillator (i.e. a swing stick on the support by two rubber pads) to the robotic arm or wrist. While a drumming machine [5] with a voice coil motor can fast beat a drum right beneath it, the beating action by a robotic drummer[6], [7], [8] is more fascinating to the audience. Execution of fast drum rolls remains a challenge to most robotic arms[7] because a larger arm swing is often at the expense of a slower beat. For example, the recently developed Disney telepresence robotic arm only managed the 4Hz desk drumming despite being equipped with powerful hybrid hydrostatic transmission [6]. While hydraulic drive worked well for this stationary arm, the heavy and bulky hydraulic compressor and the pressure tank behind the scene limit its portal use, not to mention the fluid transmission tube that stiffens the robotic arm to some extent.

What else actuators can ballistically drive a lightweight robotic drummer? To drive a drumstick, a suitable actuator needs to produce a comparably large stroke, at an adequate force and high speed. Dielectric elastomer actuator, which features high power density[9], [10], stands a great chance as the human muscle replacement. Earlier development of DEA had powered a forceful wrestling arm against a human opponent[11]; their agonist-antagonist pair also swung a leverage arm for a large swing stroke[12]. Yet, the viscoelasticity of soft dielectric elastomer was thought to limit the response speed. On the contrary, the viscoelastic human muscles that stiffen upon contraction can act ballistically. Being a stretched rubbery capacitor, DEA can store a large amount of strain energy and release part of it upon electrostatic activation. Could the highly pre-stretched dielectric elastomer act fast enough upon sudden electrostatic activation? Due to the stretch-stiffening effect[13], highly pre-stretched DEA could act fast by recoil.

Earlier designs of DEAs focused on maximizing the displacement generation [14] but few on maximizing the force induction. While a stack of multiple dielectric elastomer layers helps accumulate the forces[15], [16], the increased mass slows down the action. Similarly, earlier studies on time response were limited to actuation stroke [17] but not force. To date, the DEA still cannot simultaneously meet the need

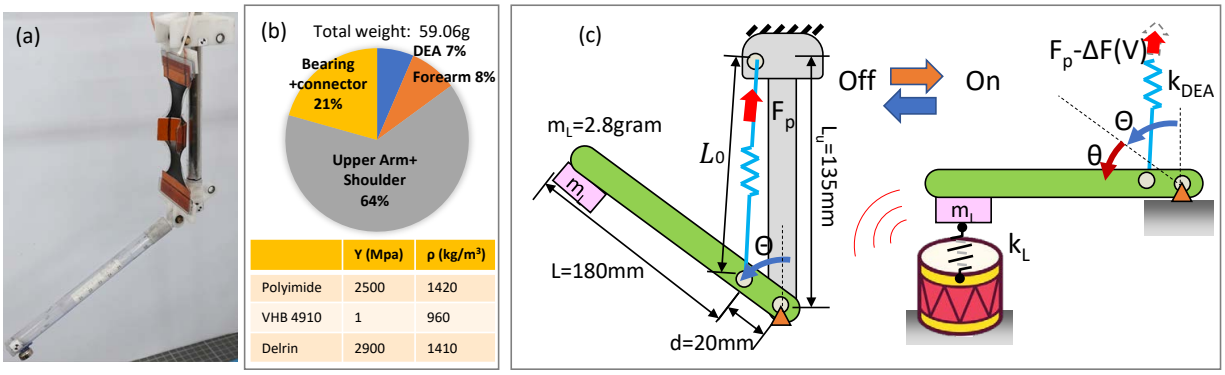

Fig. 1. A robotic drummer using dielectric elastomer actuators: (a) photographs of prototype, (b) weight component and constituent material properties; (c) a model of a spring supported leverage

for speed, stroke, and force. Fast drive by DEA was often at the expenditure of a reduced stroke and its application was thus limited to miniaturized robotic systems [18]. Based on the above review, several ways are foreseen feasible to address the need for a fast robotic drummer as shown in Figure 1, namely firstly by reducing the forearm inertia to match the DEA stiffness, secondly by finding a harder dielectric elastomer, and thirdly by adding passive elasticity to the current dielectric elastomer. The combination of a lightweight forearm and elastically reinforced DEA stand a good chance for fast action, without material change.

Recently, we showed that a long strip of highly pre-stretched DEA can be reinforced with a flexible frame to make a bowtie series with extra elasticity so that it acted faster than a pure-shear series of lightly pre-stretched DEA [19]. However, the force output by this minimum energy structure was limited because the induced force was expended to unbuckle the longitudinal flanges of the reinforcing frame. It was wondered if the lateral flexural elasticity can help a fast recoil without sacrificing the longitudinal stroke. Here, we proposed and tested a new design of double-saddle DEA as shown in Figure 1a. It consisted of two electrode segments that relaxed into a saddle shape following the laterally buckled beam. This double-saddle DEA can be completely flattened by ultimate actuation, transforming the mode of deformation from uniaxial to pure-shear. We shall investigate how fast a DEA can induce an isometric stress change. We shall show that the speed of isometric force induction is most critical in the drive of a drumstick. Finally, we shall present the demonstration, speed, and impact test of a DEA-driven drumstick.

II. Principle and Design

To act fast, the simplest drumming robot was designed to be ultra-lightweight. It consisted of a lightweight drumstick pivoted at a distal end O and a long strip of dielectric elastomer actuator at the position of the biceps. It can be modeled as a lever with a spring support, albeit the spring tension is voltage-modulated.

A. Arm Design and System Dynamics

Here, we have a drumstick made of a plastic tube of m_d =5-gram weight and L =200mm long. To further increase the impact for drumming, the tip of the drum stick is loaded with a m_L =2.8 gram metal piece. The tube was pivoted to an elbow joint (i.e. a plastic connector) O of 15-gram at the end of the upper arm. A long strip of DEA was attached at the bicipital position via a bearing-supported plate at a close distance of d =20mm off the pivot. This configuration of DEA-supported drumstick presents a leverage ratio of 10 at the tip of the drumstick. When swinging freely, this DEA-driven drumstick has the dynamic angular motion governed by the equation of motion:

$$J_O\ddot{\theta} + k_{DEA}d^2\theta = \Delta F(V)d, \tag{1}$$

where θ is the dynamic angular displacement off the static equilibrium position Θ where the static moments balance: $k_{DEA}d^2\Theta = m_dgL/2 + m_LgL$. The moment contribution by the DEA of linear stiffness k_{DEA} is angle-dependent stiffness due to its inclination concerning the arm $\approx \Theta$. This drumstick rotates counter-clockwise when the tension in the DEA reduces with increasing the applied voltage V. The voltage-induced tension decrement is denoted as $\Delta F(V)$. Upon hitting the tip of the drumstick on the drum, the depressed drum membrane provides extra elasticity to the bouncing tip before separation. Then, the drumstick's equation of motion becomes:

$$J_O\ddot{\theta} + k_{DEA}d^2\theta + k_{drum}L^2\theta = \Delta F(V)d. \tag{2}$$

If the DEA remains activated, the drumstick may bounce off the recoiling drum surface and subsequently fall freely. Following Equation (1), it bounces and falls back to make a second hit onto the drum. However, if the DEA was switched off, the drumstick was pulled higher up to a passive equilibrium position. The deactivated oscillation follows the equation of dynamic motion below:

$$J_O\ddot{\theta} + k_{DEA}d^2\theta = 0, \tag{3}$$

subjected to respective initial conditions. Based on this linear model, the system's natural frequency is f_n =

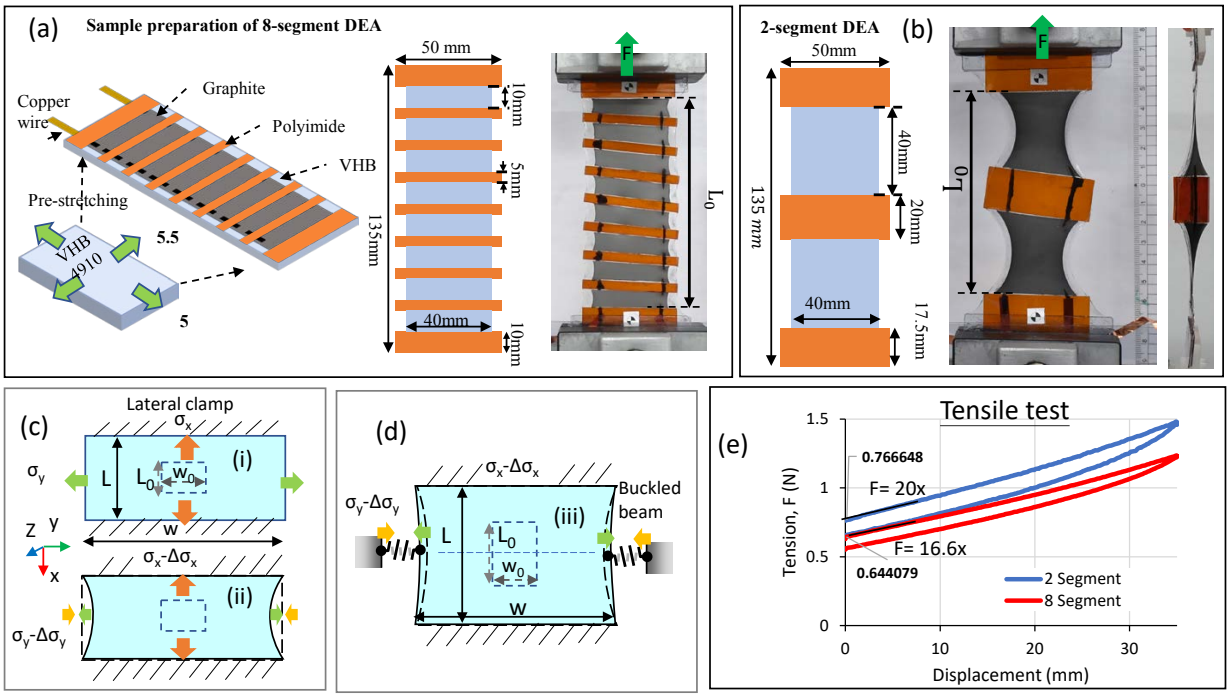

Fig. 2. Novel DEA designs and their tensile test: (a) A reference design of a 8-segment DEA (pure-shear series) and its fabrication step, (b) a proposed double-saddle DEA (with a lateral flexure), (c) a reference model of the pure-shear DEA and (d) a model of the lateral-spring-supported DEA, (e) tensile testing of the above-mentioned DEA membranes.

$(1/2\pi)\sqrt{k_{DEA}d^2/J_o}$. The natural frequency was calculated to be 1.05Hz upon substituting the following parameters: m_L=2.8g, m_d=5g, L=0.2m, d=0.02m, $J_O = m_L L^2 + m_d L^2/3 = 1.79 \times 10^{-4} kgm^2$, and k_{DEA}=20N/m.

B. Design of Double-Saddle DEA

Figure 2 shows methods of lateral reinforcement for a long strip of a highly pre-stretched DEA. There are two extreme designs of lateral reinforcement, either none or full clamp. A uniaxial DEA (as shown in Ref. [19]) under a longitudinal pre-load is prone to necking due to the lack of lateral reinforcement once the pre-stretched dielectric elastomer membrane is released. This relaxed DEA thickens and softens, and becomes susceptible to premature failure. In comparison, a standard pure-shear series as shown in Figure 2a has the pre-stretched membrane kept taut and thin by lateral reinforcement strips that divide the long membrane into multiple short ones. As a result of lateral restraint, this highly pre-stretched DEA can withstand a greater breakdown voltage. Further, the voltage-induced areal expansion of these short DEA series was concentrated in the longitudinal direction.

Figure 2b shows our novel proposal of using a flexible reinforcement beam to divide a long strip of highly pre-stretched dielectric elastomer membrane and buckle it into a double-saddle shape. Such a double-saddle DEA relaxed laterally and popped out-of-plane, unlike the flat forms of either taut pure-shear DEA or a relaxed uniaxial DEA. The laterally buckled beam provides flexural elasticity and forms the pre-stretched dielectric elastomer membrane into saddle shapes. Interestingly, the ultimate electrostatic compression eventually unbuckles the lateral beam and flattens the dielectric elastomer, transforming to a pure-shear-like ultimate actuation.

Let us analyze the isometric test of a DEA and calculate the maximum blocked force induced. The isometric force induction depends on the maximum electrostatic pressure and the hydrostatic force transmission to the longitudinally direction. Here, we shall find the effect of a lateral spring (i.e. the buckled beam) on the isometric force induction. Like a short pure-shear DEA as shown in Figure 2c, a solid part of two-saddle DEA become nearly flattened upon ultimate actuation but a lateral spring support as shown in Figure 2d. The pre-stretched geometry of this solid is w wide and L long. Its voltage-induced incremental deformation follows the three-dimensional Hooke's law[20]:

$$\Delta e_x = \frac{\Delta\sigma_x}{Y} - \frac{\nu}{Y}(\Delta\sigma_x + \Delta\sigma_z) \quad (4)$$

$$\Delta e_y = \frac{\Delta\sigma_y}{Y} - \frac{\nu}{Y}(\Delta\sigma_y + \Delta\sigma_z) \quad (5)$$

$$\Delta e_z = \frac{\Delta\sigma_z}{Y} - \frac{\nu}{Y}(\Delta\sigma_x + \Delta\sigma_y) \quad (6)$$

where Δe_i and $\Delta\sigma_i$ stand for the incremental strain and stress induced by the voltage activation and the subscript i are the indices for x, y, z directions along the length L (longitudinal), width w (lateral) and thickness respectively.

Given that the lateral stress balance between the buckled beam and dielectric elastomer membrane, the lateral membrane stress change follows: $\Delta\sigma_y = (k_{PI}w/L)\Delta e_y$, where k_{PI} is the spring constant of the middle laterally

buckled beam. Then, the isometric stress change due to the application of electrostatic pressure is derived as

$$\Delta\sigma_x = \nu\Delta\sigma_y - \nu p_e, \tag{7}$$

upon substituting Equation (7) with the following loading and boundary conditions: $\Delta e_x = 0$ for the isometric condition in the longitudinal direction and $\Delta\sigma_z = -p_e$ for the compressive loading in the thickness direction. This expression shows that the laterally buckled beam provides a boost to the lateral pre-tension against the membrane relaxation. This extra pre-tension can increase the limit of dielectric breakdown but needs not undermine the ultimate active force decrement. In the limiting case where the lateral beam was ultimately flattened, the flattened DEA hardly expanded laterally $\Delta e_y = 0$ and it thus produced as much isometric stress as the pure-shear DEA following the expression: $\Delta\sigma_x = \nu p_e/(1-\nu)$.

C. Sample preparation and tensile test

Figure 2a shows the fabrication steps for dielectric elastomer actuators with reinforcement. The two reinforced designs are a pure-shear series with 8 electrode segments and a two-saddle DEA with two electrode segments. First, we pre-stretched a piece of VHB 4910 adhesive tape (3M, 1mm thick) biaxially ($\lambda_{px} = L/L_0$=5 times longitudinally and $\lambda_{py} = w/w_0$ =5.5 times laterally) and bonded the stretched membrane to a rigid frame. Second, we patterned compliant electrodes by brushing graphite powder on both sides of the stretched membrane. The total electrode area for both DEA designs was kept the same at 3200 mm^2. For example, each electrode for two saddles DEAs is 40mm wide and 40mm long; each electrode for an 8-segment pure-shear series is 40mm wide and 10mm long. Third, we applied copper foils to connect the graphite electrodes via the carbon-grease contact. Finally, we reinforced the long strip of electrode-clad stretched membrane with a 0.125mm thick polyimide plate or beam. In making a pure-shear series, eight pieces of polyimide plate each 50mm wide and 7mm long were applied on one side of the pre-stretched dielectric membrane. In making a double-saddle DEA, only a middle reinforcement beam of 50mm wide and 20mm long was applied. This double-saddle DEA weighed merely 4.5 grams.

The two DEA designs differ in pre-tension requirement. A tensile tester (Cometech QC-513MF) was used to load and unload the DEA samples. The starting pre-stretch was 5 times the non-stretch length and the final stretch was 7.15 times. Both samples are subjected to a hysteresis when being loaded and unloaded for a cycle at a stretch rate of 0.5 mm/s. Figure 2 show that the double-saddle DEA was stiffer and required more pretension for the same pre-stretch as compared to pure-shear series. The stiffness of double saddle DEA was 20.0N/m, 20% greater than 16.6N of the 8-segment DEA. The pretension for 5-times pre-stretching the double-saddle DEA was 0.767N, 19% greater than 0.644N required for the same-pre-stretched 8-segment DEA. At first sight, it was puzzled why the more relaxed double-saddle DEA was stiffer than the flat and taut pure-shear series. Indeed the double saddle did not relax as much as the projected view but simply curled. Its enhanced longitudinal tension was contributed by the lateral buckled spring as predicted by the theory above (Equation 7).

III. Results and Discussions

This section covers the test of actuators, a free swing of a DEA-driven drumstick and finally the drumming demonstration.

A. Pulsed isotonic test

First, the above DEAs were subjected to isotonic tests as shown in Figure 3. The DEA each under isotonic test carried a pre-load that stretched the active membrane 4.25 times longitudinally. The preload for a double-saddle DEA was 61 grams, and that for an 8-segment pure-shear series was 56 grams. When activated by high voltage, the DEAs elongated and lowered the pre-load (as shown in Figure 3a-c). To study the voltage-dependent time response, the DEA under test was subjected to a stepwise pulse activation where a voltage pulse of 20s pulse width (10s on and 10s off) was modulated by a stepwise voltage ramp at 0.5kV steps up to 7kV. A high-voltage supply/amplifier (Trek 610E with a maximum 10kV DC voltage and 1.2kHz bandwidth) was used to provide the high-voltage pulses.

Figure 3a-b shows that the activated membrane of DEA thinned down and elongated. In addition, we observed secondary effect in the activated DEAs. For example, the initially buckled double-saddle DEA, together with the middle beam, become flattened when activated. On the other hand, the necking (waistline) of pre-stretched membrane reduces when the 8-segment DEA was activated. Figure 3c shows the time plot of isotonic extension; whereas, Figure 3d shows the active stroke and return stroke as a function of driving voltage. It noted that the ultimate actuation by double saddle DEA was around 20mm as much as that achieved by the 8-segment pure-shear series. This confirmed the beneficial transition of double-saddle DEA from uniaxial actuation to pure-shear one.

Figure 3d shows the active stroke and strain as a function of driving voltage. At lower voltages of the ramp, the active stroke (strain also) appeared as a quadratic function of voltage, but it tapered to a plateau at a higher voltage. Over this tapered regime of actuation, the DEA was believed to be strain stiffened under over-compression. Interestingly, Figure 3c shows that the rise time of the over-compressed double saddle DEA decreased with increasing the voltage. For example, Figure 3e(iii) show that the double-saddle DEA can return faster (with a down time of 0.81s) upon deactivation from the 7kV ultimate actuation. This down time of return was 0.81s, being one third spent by the 8-segment counterpart. This speedy return is attributed to the additional elasticity of middle buckled beam.

Table 1 compares the isotonic performance among various DEA types. This work shows that lateral reinforcement helps keep a large pre-stretch in a long strip of DEA, increasing

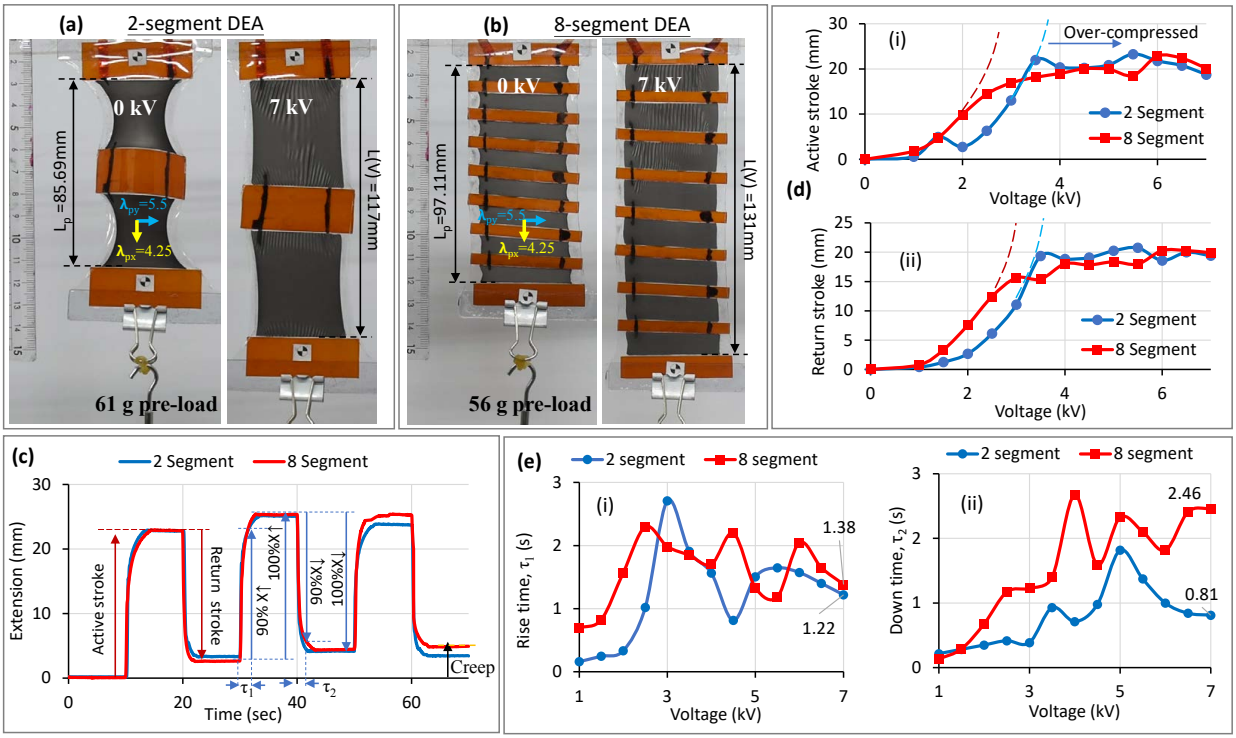

Fig. 3. Isotonic test of DEAs carrying a pre-load: (a) photographs of a double saddle DEA tested ; (b) photographs of an 8-segment DEA tested; (c) the stepwise pulsed activation (modulated by a voltage ramp from 6kV to 7kV); (d) the (i) active and (ii) return strokes as the function of the driving voltage; (e) the (i) rise and (ii) down times as a function of step activation voltage

TABLE I
ISOTONIC PERFORMANCE COMPARISON AMONG VARIOUS DEAS

Parameter	multi-layered stack [10]	uniaxial strip [19]	8-segment DEA	2-segment DEA (new)
Preload	1000g	50.15g	56g	61g
Actuator weight	20g	2g	3.39g	4.48g
Actuator length	107mm	63mm	97.1mm	85.7mm
Material	Acrylic elastomer	VHB 4910	VHB 4910	VHB 4910
Pre-stretch	-	5.5×5	5.5×4.25	5.5×4.25
Ultimate voltage	3.5kV	4.5kV	7kV	7kV
Isotonic stroke	12.5mm	5.96mm	22.9mm	23.3mm
Isotonic strain	19.8%	6.25%	33.6%	34.2%
Work density	3.92J/kg	1.46J/kg	3.7 J/kg	3.2 J/kg
Isotonic Rise time	2.0s	1.95s	1.38s	1.22s
Isotonic Down time	2.0s	0.917s	2.46s	0.81s

the preload and ultimate isotonic strain. The lateral reinforcement of a highly pre-stretched dielectric elastomer warranted a higher breakdown field and interesting leads to faster time response.

B. Pulsed isometric response

Next, we study how fast a blocked force can be induced by a DEA during the isometric test which has the activated actuator fixed in length. Figure 4 shows that the samples of DEAs were pre-stretched 5 times and mounted to a tensile tester when they were activated by a stepwise pulse train for 10 s and deactivation for 20 s. When being inactive, the sample under test was subjected to a constant pre-tension. As the actuator length was fixed, the step activation by electrostatic pressure reduced the actuator's longitudinal tension and simultaneously caused a slight lateral expansion beyond the necking sides as shown in Figure 4a-b.

Figure 4c-d shows that these isometrically induced tension decrements appeared as a quadratic function of voltage, up to a threshold voltage beyond which the active tension change reached a plateau with increasing voltage due to the severe membrane wrinkling. Figures 4d and 4e show that the double saddle DEA produced nearly 15% less ultimate isometric tension decrement than the 8-segment DEAs, but it responded faster for ultimate activation and deactivation. Then, the former's ultimate rise time at 5-7kV was approximately 0.5s, and its ultimate downtime was between 0.77 to 0.85s. In comparison, the 8-segment DEA had an ultimate rise time above 1s and ultimate down time around 5.0s. This slow response could be attributed to the high relaxation in the over-bounded and locally wrinkled.

Interestingly, the less bounded and lightly relaxed membrane of the double-saddle did not suffer from the same speed limit when activated near the ultimate voltage. With the help of embedded flexural elasticity in a double-saddle DEA, a faster-than-expected induction of ultimate isometric force was realized and promises a faster drive of 'soft' robots.

C. Free Arm Swing

Figure 5 shows a free-swing test for a DEA-driven drumstick. Figure 5a shows that the inactive DEA raised the

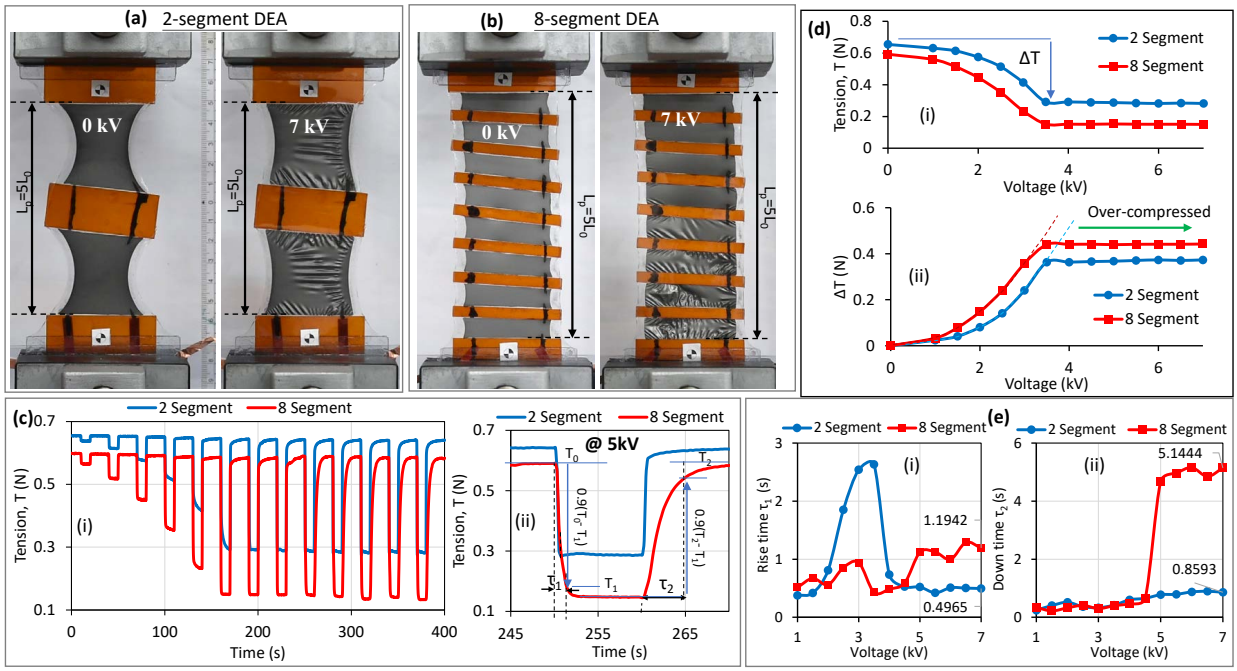

Fig. 4. Isometric test of DEAs at a fixed length: (a) photographs of a double saddle DEA; (b) photographs of an 8-segment DEA; (c) the isometric tension changes with stepwise pulse activation; (d) (i) the isometric tension T and (ii) tension decrement (ΔT) as a function of the applied voltage; (e) the (i) rise and and (ii) down times as a function of driving voltage.

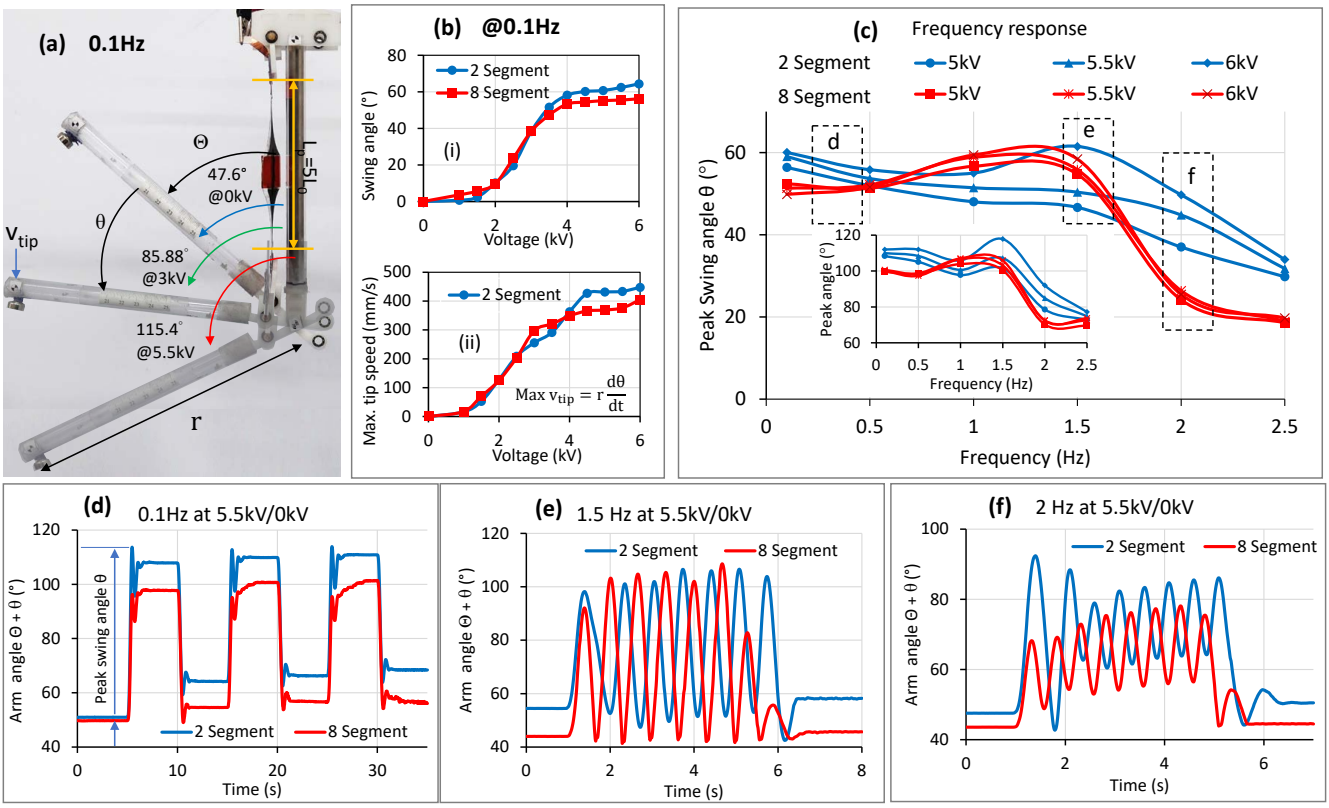

Fig. 5. Free swing of a DEA-driven drumstick: (a) overlay of activated swing positions at middle and low; (b) the angular swing position (off the vertical line) and the tip speed as a function of pulsed voltage amplitude; (c) frequency response of peak swing angle or peak angle; (d)-(f) time response of the pulsed activation at 0.1Hz, 1.5Hz and 2 Hz.

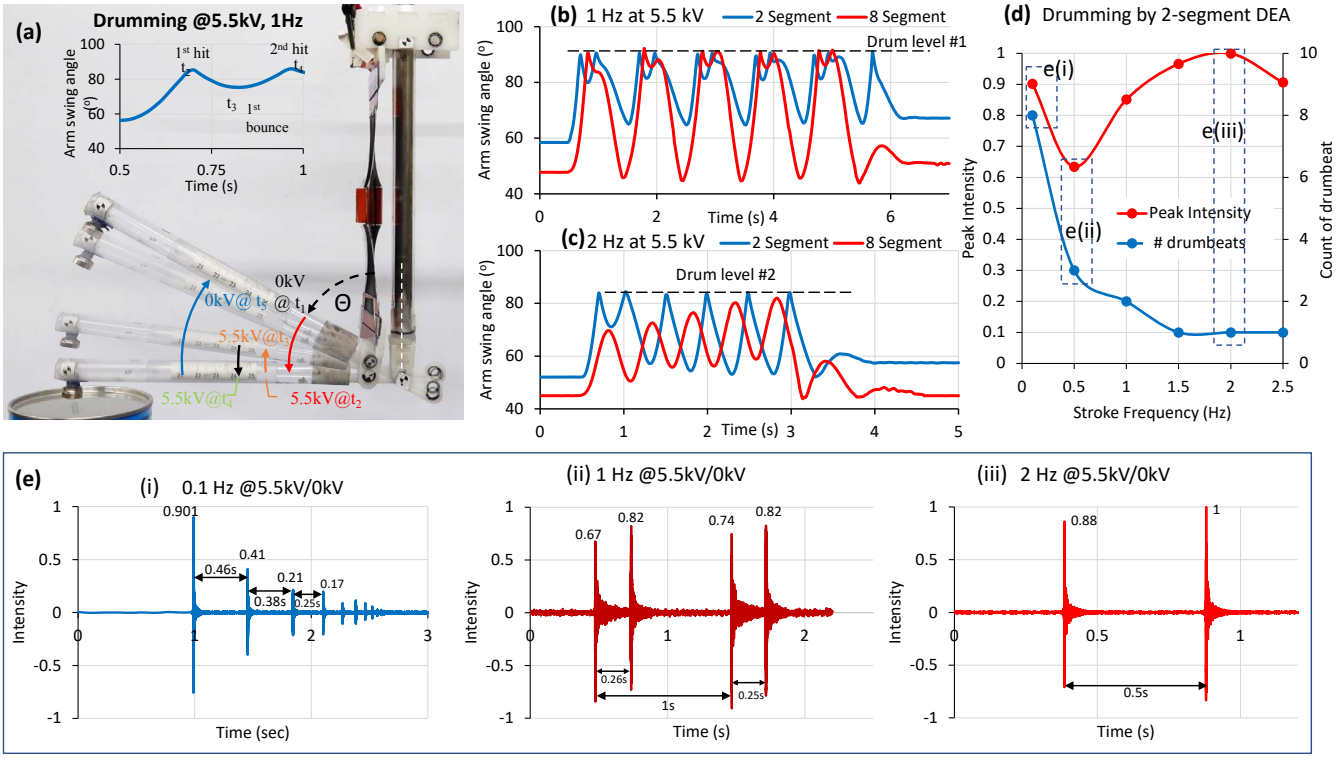

Fig. 6. Demonstration of drumming: (a) overlay of photographs showing the major hit and bounces upon 5.5kV activation for 1 Hz; (b)-(c) Drum beating by 2-segment and 8-segment DEA for 1 Hz and 2Hz pulse (5.5kV voltage) respectively ; (d) number and loudness of drumbeat under the drive by double-saddle DEA; (e) the sound intensity generated by the double-saddle-DEA-driven drumstick at 0.1Hz, 1Hz, and 2Hz.

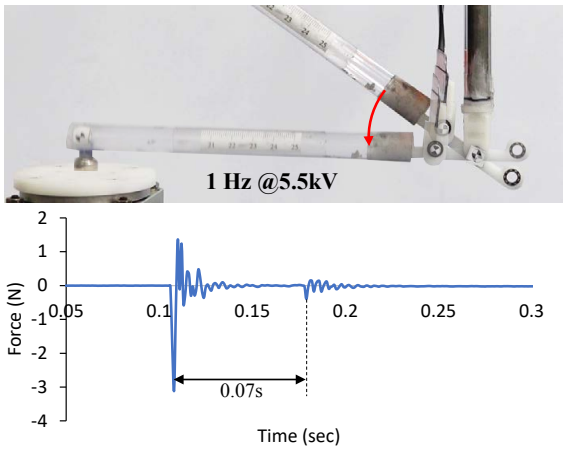

Fig. 7. The blocked force measurement; the drumstick hit on the drum and bounces when DEA pulsed at 5.5kV for 1s stroke interval.

drumstick resting high at $\Theta = \theta(0) = 47.6°$ off the upper-arm rod. When the DEA was activated with a 10s-wide pulse, the drumstick fell and swung eventually to a steady-state on position. When the pulse was switched off, the DEA shortened and pulled up the once-lowered drumstick. This recoil was followed by an overshot above and a fall below the passive neutral height that creeps lower over cycles.

Figure 5b shows the peak swing angle $\theta(V)$ increasing as a quadratic function of voltage up to 3kV beyond which the actuation tapered. A similar trend was observed for the peak tip speed of the swung arm. Interestingly, the DEA-driven drumstick managed to swing the tip as fast as 447mm/s upon a 6kV pulsed activation, breaking the earlier speed record of DEA-driven arm[10].

Figure 5c shows the frequency response of the peak swing angle, whereas Figure 5d-f shows the time response of the arm angle upon the DEA's pulsed activation. It is noted that the swing angle of the DEA-driven arm stayed nearly constant (increased or decreased slightly) up to 1.5Hz pulse frequency, beyond which the swing angle decreased substantially. Figure 5d shows that the 0.1Hz pulsed activation of DEA resulted in a sudden fall of the once DEA-supported arm with an overshoot in arm swing. When the pulse was off, the arm did not fully return to the starting position due to the DEA's creep. When activated faster than the resonant frequency, the swing angle decreases with increasing pulsed frequency and so does the creep. Yet, the double-saddle DEA performed dynamically better than the pure-shear series. The former swung a larger angle than the 8-segment one, suffering lesser from dynamic stroke decrement.

D. Drumming Demonstration

Next, we compared two DEAs for driving the robotic drummers. Figure 6a shows a tin drum placed between $\theta + \Theta = 80 \sim 90°$ with the reach by a DEA-driven drumstick. When activated at 0.1Hz, both DEAs, double saddle and 8-segment, can hit the drum with the reach

with multiple bounces. However, as the pulsed frequency increased, the stroke amplitude decreased and so did the number of bounces. Figure 6b shows that a double saddle DEA excited two drumbeats per 1Hz stroke under the 5.5kV pulsed activation, whereas it excited one drum beat per 2Hz stroke. In comparison, the 8-segment DEA managed two drumbeats per 1Hz stroke but missed to beat per 2Hz stroke.

Figure 7 shows that the first impact force for the 1Hz pulsed activation of double-saddle DEA was as high as 3.1N. Figure 6d summarizes the number and loudness of drumbeats as a function of stroke frequency. The number of drumbeats decreases down to 1 with increasing the stroke frequency above 1.5 Hz. However, there is an optimum stroke frequency near 2 Hz to maximize the loudness of the drumbeat. Figure 5e shows that a 0.1Hz stroke by 5.5kV activation excites 8 drumbeats per stroke while a 2Hz stroke excites only a drumbeat per stroke. These 8 drum rolls for a 0.1Hz stroke were rather fast: the interval between the fourth and third drumbeat was as short as 0.16 seconds. After all, the total number of drum rolls per pulse-width did not exceed the maximum stroke frequency. Due to energy dissipation, the loudness of drumbeats diminished over bounces after a power stroke. For example, the loudness of the fourth drumbeat fades to 0.17, in comparison to 0.9 of the first drumbeat for a 0.1Hz stroke.

IV. Conclusions

In short, the actuation of dielectric elastomer may taper and depart from a quadratic rise when activated at a very high voltage. This tapered actuation may be detrimental to the large-stroke requirement, but interestingly it was found to improve the speed of isometric force induction. To further increase the speed of force induction, we introduced a buckled beam as the lateral reinforcement to a two-segment DEA, forming a double-saddle DEA. This additional flexural spring may decrease the active isometric stress change but interestingly improved the action and return speed near the ultimate actuation of dielectric elastomer. Here, we found that the ultimate actuation of double-saddle DEA can be pulsed faster for force exertion than that of a 8-segment DEA. As such, a double-saddle DEA can drive a robotic drummer faster at lesser dynamic stroke decrement than the latter.

In addition, we found the DEA-driven drummer can generate multiple drumbeats after a power stroke. These consecutive bounces happen because of drumstick oscillation. In addition, it was noted that the voltage-induced creep over cycles eventually increases the number of bounces. These interplays between stroke, force and speed make the master of drum rolls complex for a simple robotic drummer under a constant pulsed activation. It is foreseen that a harder dielectric elastomer material[13] promises to drive a robotic drummer faster to match a human drummer.

ACKNOWLEDGMENT

The first authors acknowledged the scholarship from the International College of Semiconductor Technology, National Yang Ming Chiao Tung University (NYCU). The authors acknowledged the support from the National Science and Technology Council (grant number MOST 109-2628-E-009-012-MY3 and NSTC 112-2221-E-A49-140). The corresponding author G.-K.L. acknowledges the support by the Higher Education Sprout Project of the NYCU and Ministry of Education (MOE), Taiwan.

References

[1] S. Atwal, "World's fastest drummer: 11-year-old from australia breaks record," https://kids.guinnessworldrecords.com, 2022, [Accessed 16-08-2023].

[2] A. Z. Hajian, D. S. Sanchez, and R. D. Howe, "Drum roll: Increasing bandwidth through passive impedance modulation," in *Proceedings of International Conference on Robotics and Automation*, vol. 3. IEEE, 1997, pp. 2294–2299.

[3] M. M. Williamson, "Robot arm control exploiting natural dynamics," Ph.D. dissertation, Massachusetts Institute of Technology, 1999.

[4] A. Kapur, "A history of robotic musical instruments," in *ICMC*, vol. 10, no. 1.88, 2005, p. 4599.

[5] Polyend.com, "Polyend perc: Drumming machine," https://polyend.com/legacy/polyend-perc/, Aug 2022.

[6] J. P. Whitney, T. Chen, J. Mars, and J. K. Hodgins, "A hybrid hydrostatic transmission and human-safe haptic telepresence robot," in *2016 IEEE international conference on robotics and automation (ICRA)*. IEEE, 2016, pp. 690–695.

[7] N. J. Stanford, "Automatica - robot drummer tests," https://www.youtube.com/watch?v=qPT0TNj-YRk, September 2017, [Accessed 16-08-2023].

[8] E. ACKERMAN, "Xiaomi's humanoid drummer beats expectations," https://spectrum.ieee.org/xiaomi-robot-drummer, December 2022, [Accessed 16-08-2023].

[9] R. Pelrine, R. Kornbluh, J. Joseph, R. Heydt, Q. Pei, and S. Chiba, "High-field deformation of elastomeric dielectrics for actuators," *Materials Science and Engineering: C*, vol. 11, no. 2, pp. 89–100, 2000.

[10] M. Duduta, E. Hajiesmaili, H. Zhao, R. J. Wood, and D. R. Clarke, "Realizing the potential of dielectric elastomer artificial muscles," *Proceedings of the National Academy of Sciences*, vol. 116, no. 7, pp. 2476–2481, 2019.

[11] G. Kovacs, P. Lochmatter, and M. Wissler, "An arm wrestling robot driven by dielectric elastomer actuators," *Smart Materials and Structures*, vol. 16, no. 2, p. S306, 2007.

[12] P. Lochmatter and G. Kovacs, "Design and characterization of an active hinge segment based on soft dielectric eaps," *Sensors and Actuators A: Physical*, vol. 141, no. 2, pp. 577–587, 2008.

[13] G.-K. Lau, Z.-X. Ren, and K.-T. Chiang, "Effect of stretch limit change on hyperelastic dielectric actuation of styrene–ethylene/butylene–styrene (sebs) copolymer organogels," *Smart Materials and Structures*, vol. 31, no. 9, p. 095019, 2022.

[14] T. Lu, Z. Shi, Q. Shi, and T. Wang, "Bioinspired bicipital muscle with fiber-constrained dielectric elastomer actuator," *Extreme Mechanics Letters*, vol. 6, pp. 75–81, 2016.

[15] G. Kovacs, L. Düring, S. Michel, and G. Terrasi, "Stacked dielectric elastomer actuator for tensile force transmission," *Sensors and actuators A: Physical*, vol. 155, no. 2, pp. 299–307, 2009.

[16] S. Hau, G. Rizzello, and S. Seelecke, "A novel dielectric elastomer membrane actuator concept for high-force applications," *Extreme Mechanics Letters*, vol. 23, pp. 24–28, 2018.

[17] S. Michel, X. Q. Zhang, M. Wissler, C. Löwe, and G. Kovacs, "A comparison between silicone and acrylic elastomers as dielectric materials in electroactive polymer actuators," *Polymer international*, vol. 59, no. 3, pp. 391–399, 2010.

[18] S. Rosset and H. R. Shea, "Small, fast, and tough: Shrinking down integrated elastomer transducers," *Applied Physics Reviews*, vol. 3, no. 3, 2016.

[19] G.-K. Lau, F.-Y. Chen, and Z.-X. Ren, "Axial force transmission in flexible bowtie dielectric elastomer actuators," *Applied Physics Letters*, vol. 120, no. 1, 2022.

[20] F. Carpi, P. Chiarelli, A. Mazzoldi, and D. De Rossi, "Electromechanical characterisation of dielectric elastomer planar actuators: comparative evaluation of different electrode materials and different counterloads," *Sensors and Actuators A: Physical*, vol. 107, no. 1, pp. 85–95, 2003.